# LEVEL SET BASED FLAMELET MODELING FOR TURBULENT PREMIXED LIFTED FLAME ON LOW-SWIRL BURNER

Sungmo Kang and Yongmo Kim*

*Department of Mechanical Engineering*
*Hanyang University, Seoul 133-791, KOREA*

***10th Int. Workshop on Premixed Turbulent Flames,***
***August 12-13, 2006/ Mainz, Germany***

# Motivations

- **To investigate the turbulence-chemistry interaction, stabilization mechanism, counter-gradient diffusion, conditional transport properties, and pollutant formation in the turbulent swirling premixed lifted flames of the Low Swirl Burner.**

- **To develop the comprehensive combustion model to realistically simulate the turbulent premixed, partially premixed and nonpremixed flames encountered in the practical combustors including gas turbine combustor, furnace and burner.**

# Physical and Numerical Models

- **Density-weighted Navier-Stokes equation**
- **Standard *k*-$\varepsilon$ turbulent model**
- **PISO algorithm handling the pressure-velocity coupling**
- **Unstructured-grid finite-volume method**
- **Parallel algorithm based on PC-cluster**
- **Flamelet-based level-set approach**
- **Detailed chemical kinetics**

# Level-Set based Flamelet Approach

- **The present approach based on the premixed flame propagation mechanism, can handle the turbulent premixed flames with the stratified mixture. This requires the formulations for *G*-equation and mixture fraction (*Z*). In the level-set/flamelet procedure used in this study, *G*-equation determines the location of the premixed flame front and mixture fraction (*Z*) expresses the state of mixing**

- **In modeling the turbulent premixed flames, difficulties associated with counter-gradient diffusion can be avoided.**

# Flamelet-based Level-Set Approach (1)

The *G*-equation is introduced to describe the premixed combustion. This non-reacting scalar avoids complications associated with the counter-gradient diffusion and does not require the modeling for a source term

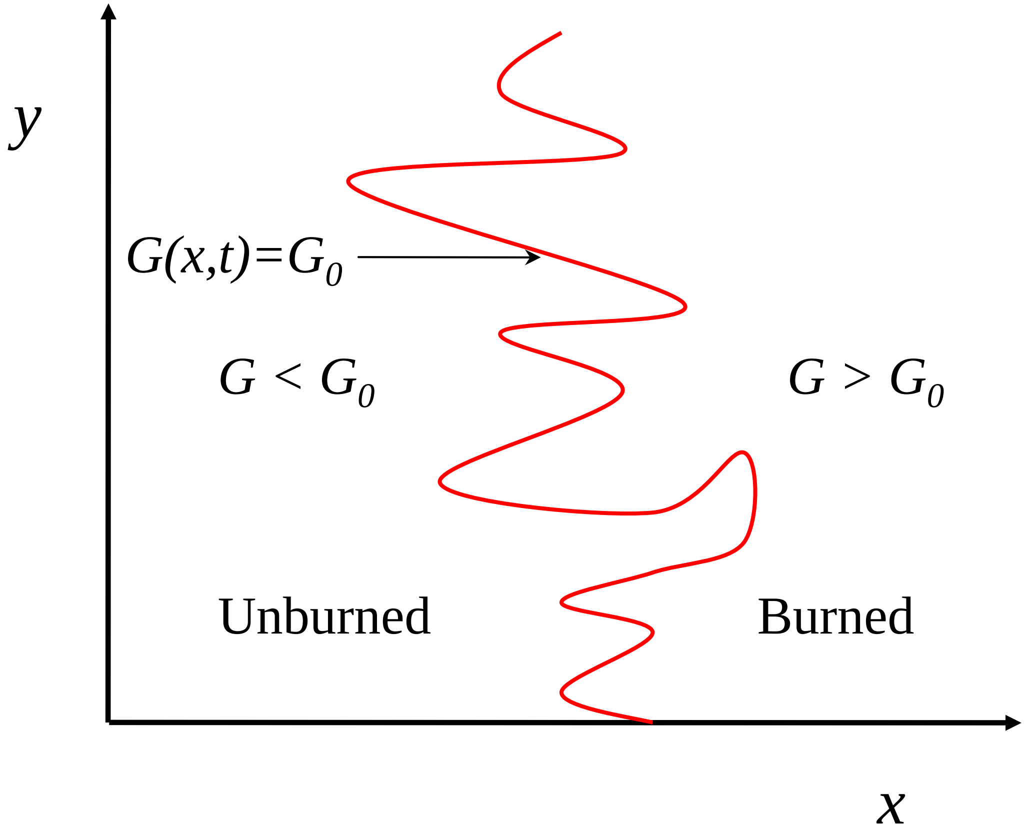

# Flamelet-based Level-Set Approach (2)

## Equation for the mean location of flame front

$$\frac{\partial\left(\bar{\rho}\tilde{G}\right)}{\partial t}+\nabla\bullet\left(\bar{\rho}\tilde{v}\tilde{G}\right)=\bar{\rho}s_{T,p}\left|\nabla\tilde{G}\right|-\bar{\rho}D_t\tilde{\kappa}\left|\nabla\tilde{G}\right|$$

where $\tilde{\kappa}$ = curvature of the mean flame front

$D_t$= turbulent diffusivity ~ *lv'*

## Equation for the variance of *G*

$$\frac{\partial\left(\bar{\rho}\widetilde{G''^2}\right)}{\partial t}+\nabla\bullet\left(\bar{\rho}\tilde{v}\widetilde{G''^2}\right)=\nabla_{||}\bullet\left(\bar{\rho}D_t\nabla_{||}\widetilde{G''^2}\right)+2\bar{\rho}D_t\left(\nabla\tilde{G}\right)^2-c_s\bar{\rho}\frac{\tilde{\varepsilon}}{\tilde{k}}\widetilde{G''^2}$$

where $\nabla_{||}$ denotes differentiation only tangential to the mean flame front

## Turbulent burning velocity (Peters, 1999)

$$\frac{s_T-s_L}{v'}=-\frac{a_4b_3^2}{2b_1}Da+\left[\left(\frac{a_4b_3^2}{2b_1}Da\right)^2+a_4b_3^2Da\right]^{1/2} \qquad Da\left(Z\right)=\frac{s_L\left(Z\right)l}{v'l_F\left(Z\right)}=\frac{s_L^2\left(Z\right)l}{v'D}$$

where $s_L$ is the laminar burning velocity, $l_F$ is a flame thickness, and constants are $a_4$=0.78, $b_1$=2.0, $b_3$=1.0

# Flamelet Library and Presumed-Shape Pdf

- Flamelet Library as a Function of $G$ and $\phi$ : $Y_i(G,\phi)$
- Presumed-Shape Pdf : Gaussian shape for $P(G)$ and Delta function for $P(\phi)$

$$\widetilde{Y}_i(x) = \int_0^{\infty}\int_{-\infty}^{\infty} Y_i((G-G_0)/\overline{\sigma}, \phi)\,\widetilde{P}(G,\phi;x)\,dG\,d\phi \quad , \quad \widetilde{P}(G;x) = \frac{1}{\sqrt{2\pi\widetilde{G''^2}}}\exp\left(-\frac{(G-\widetilde{G}(x))^2}{2\widetilde{G''^2}}\right)$$

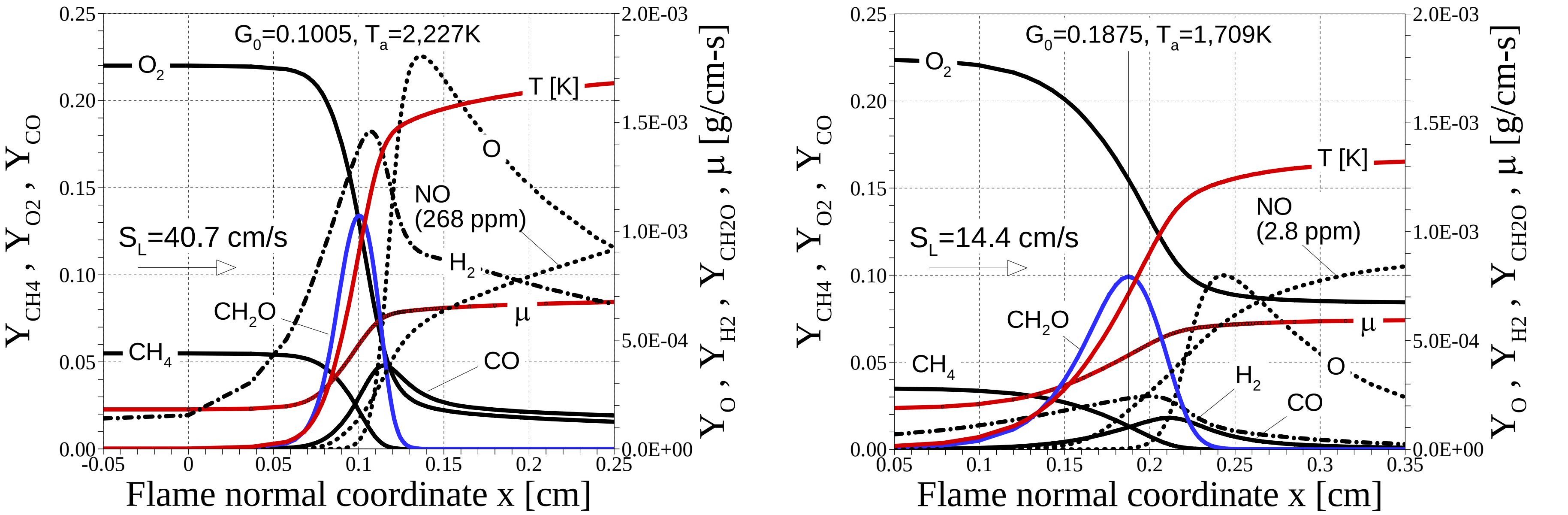


(a) $\phi$=1.0 (b) $\phi$=0.63

1-D laminar premixed flames at 1 atm and 300K using GRI-Mech 3.0 (53 species & 325 reactions). $G_0$ is defined at the peak of CH2O. Flame thickness increases as flame speed decreases.

# Validation Cases for Turbulent Premixed Lifted Flames at LSB

- ☐ **Stoichiometric-Premixed $CH_4$/Air Swirling Flame (C.K. Chan et al. 1992)**
- ☐ **Lean-Premixed $CH_4$/Air Swirling Flame ($\phi$=0.63, S. Tachibana et al. 2004)**

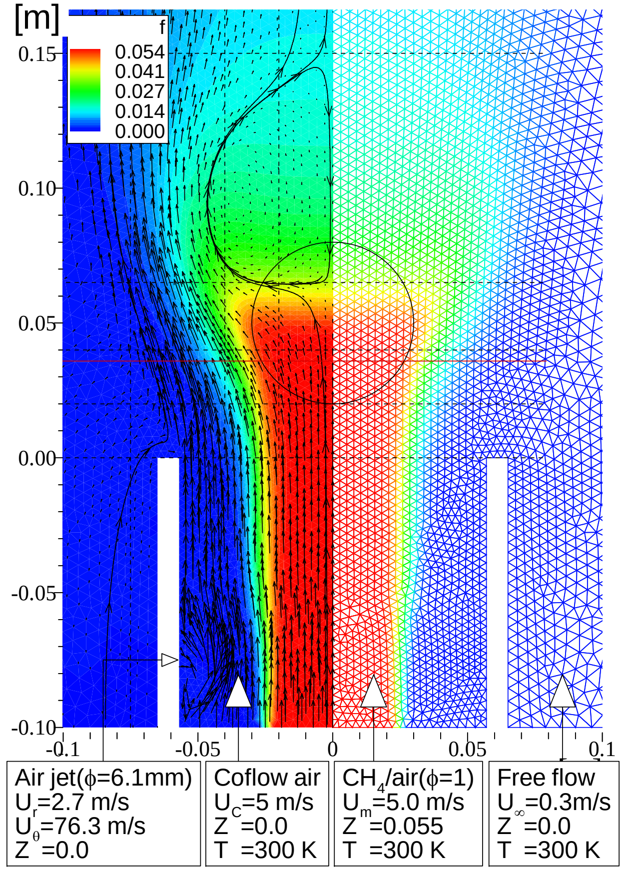


**(a) Chan's LSB (*S*=0.07, *L*=75mm, $A_j$=5mm)**

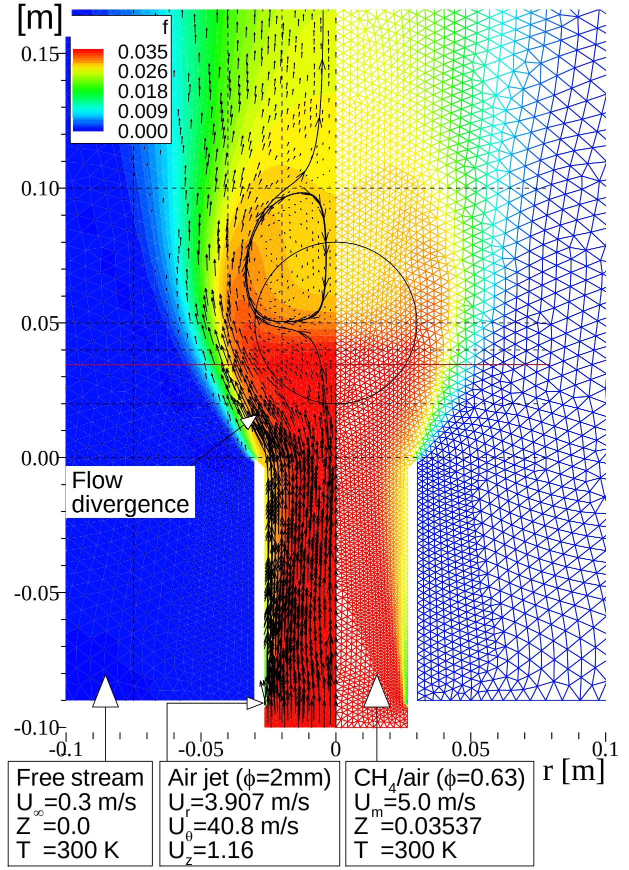


**(b) Tachibana's (*S*=1.32, *L*=90mm, $A_j$=1.64mm)**

$$S = \frac{\pi R_j R Q_j^2 \cos\alpha}{A_j (Q_j + Q_m)^2} \quad \text{or} \quad \frac{\pi R^2 Q_j^2 \cos\alpha}{A_j (Q_j + Q_m)^2}$$

# Centerline Profiles of Two Turbulent Premixed Flames

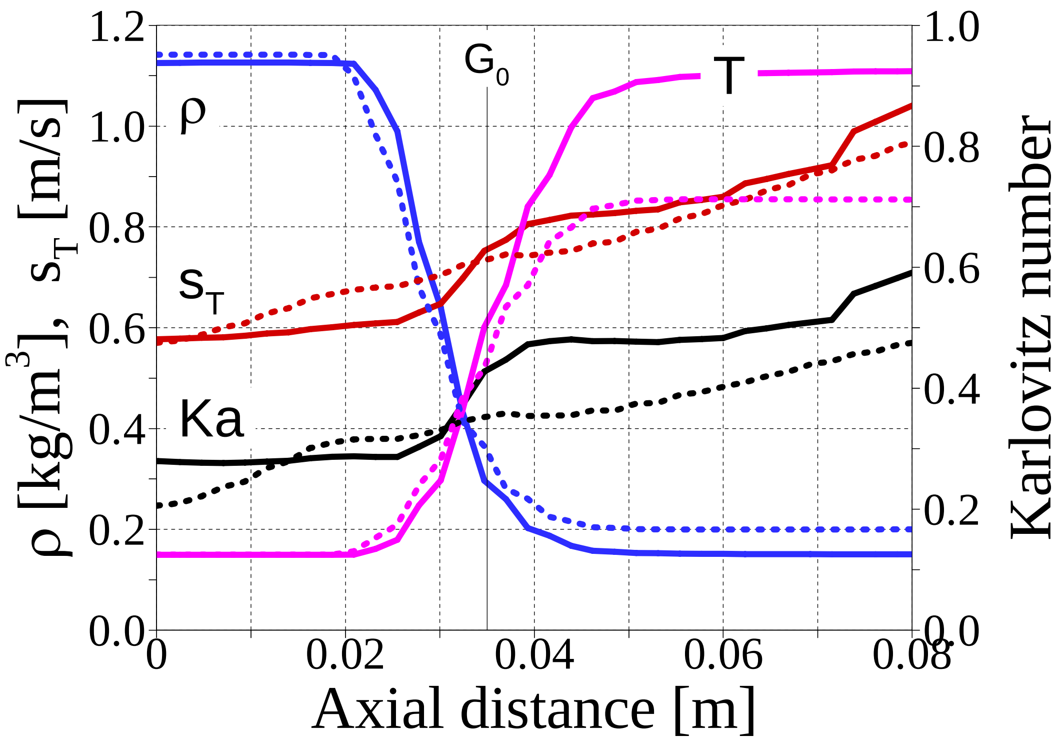


$$Ka^2 = \frac{l_F}{\eta} = \left(\frac{v'}{s_L}\right)^3 \left(\frac{l}{l_F}\right)^{-1}$$

Comparison of centerline profiles of mean density, turbulent flame speed, Karlovitz number of turbulent premixed $CH_4$/air flames in low-swirl burner. Solid lines: result for Chan's LSB ($\phi$=1.0, $S$=0.07, $L$=75 mm); dashed lines: result for Tachibana's LSB ($\phi$=0.63, $S$=1.32, $L$=90 mm).

# Turbulent Premixed $CH_4$/Air Flame (C.K. Chan et al. 1992)

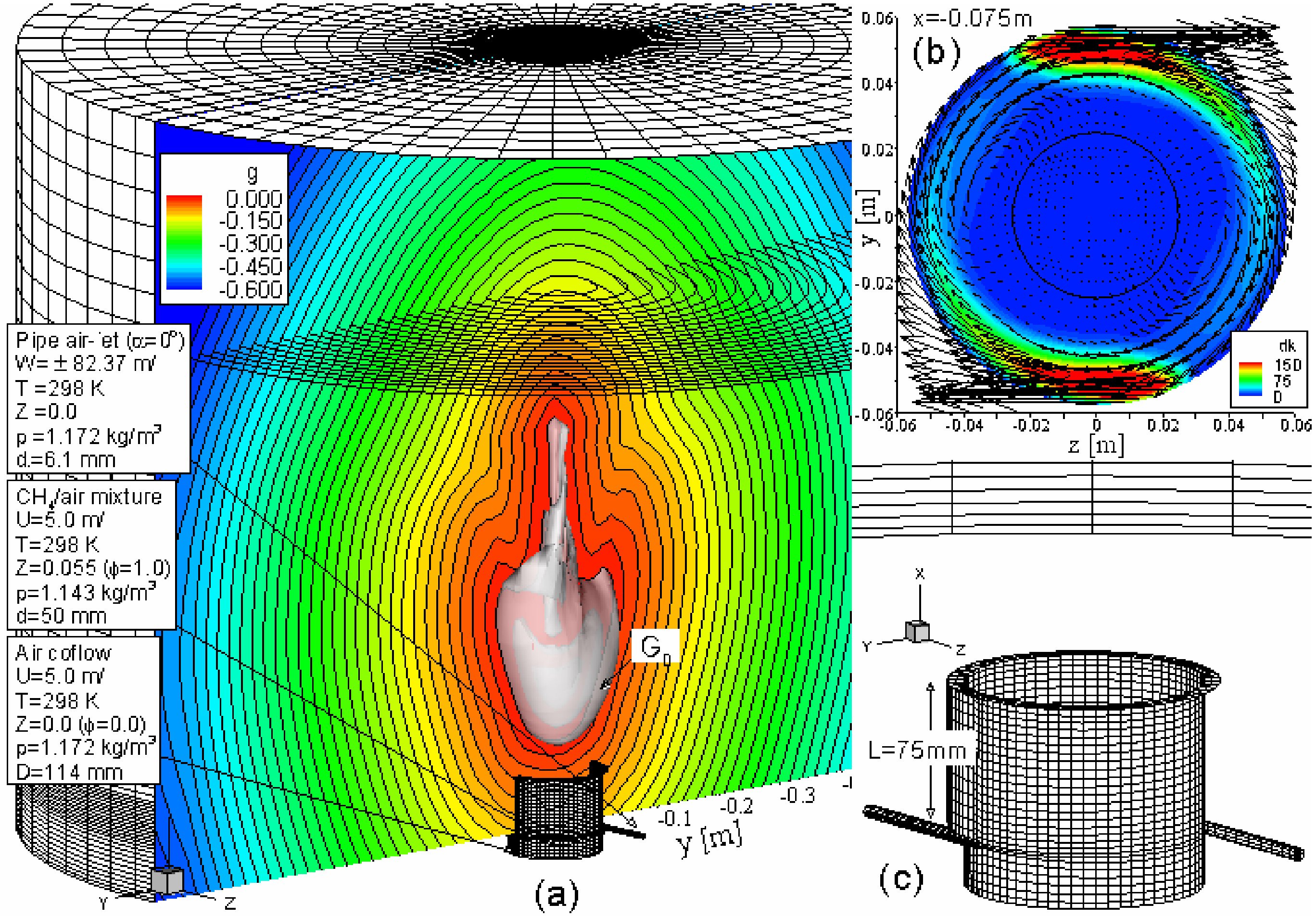


Problem configuration for turbulent premixed $CH_4$/air flame sustained by a low-swirl burner ($U_m$=5 m/s, $S$=0.07, $\Phi$=1.0, $d$=50 mm, $D$=114 mm, $D_j$=6.1 mm, rim thickness=8 mm, $L$=75 mm, ncell=139,520). (a) Inlet boundary condition & $G$-field, (b) secondary-flow vectors at the cross-section containing the air-jets, (c) blowup of burner.

# Turbulent Premixed $CH_4$/Air Flame ($\Phi$=1.0) – centerline profiles

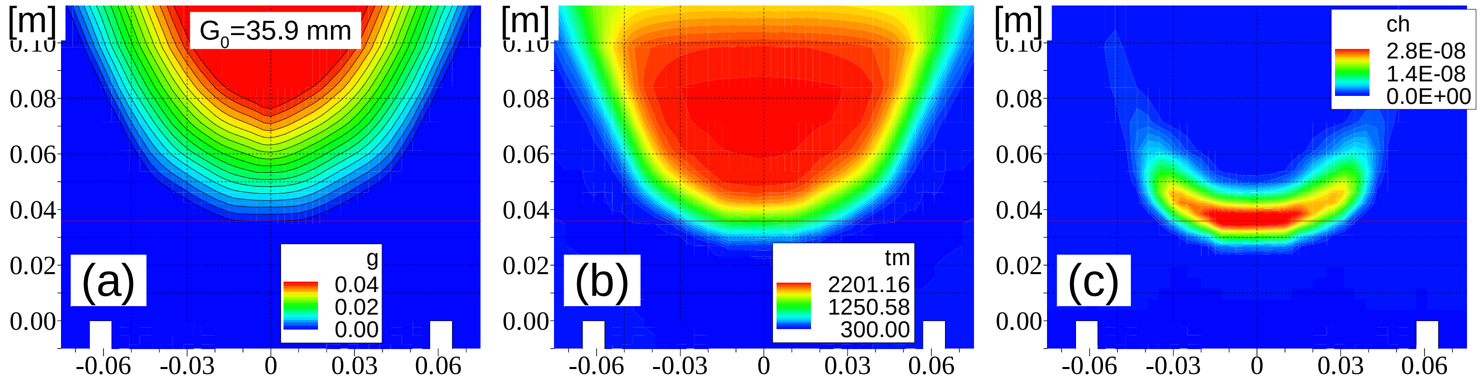


Mean flame field at centerplane of *z*=0. (a) Scalar *G*, (b) temperature, (c) CH mass fraction.

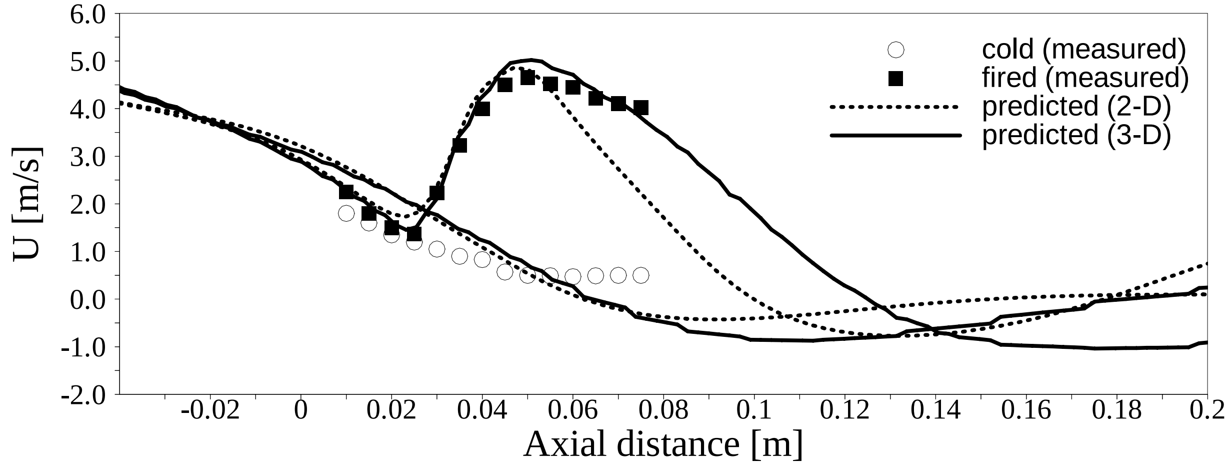


Centerline profiles of mean axial velocity ($U_m$=5 m/s, *S*=0.07 and *L*=75 mm). Symbols: Chan et al. 1992; lines: present prediction.

# Turbulent Premixed $CH_4$/Air Flame (S. Tachibana et al. 2004)

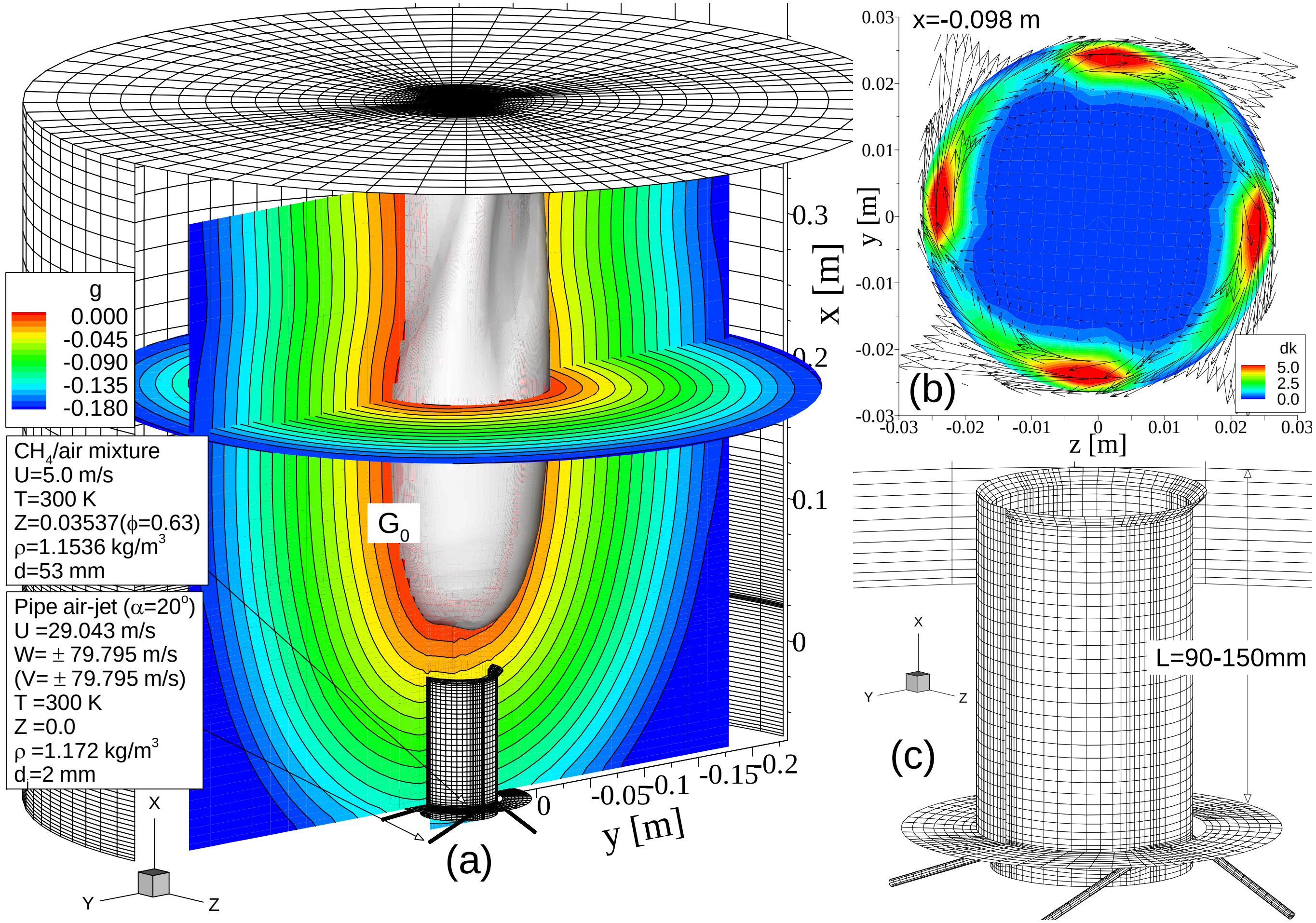


Problem configuration for turbulent premixed $CH_4$/air flame sustained by a low-swirl burner ($U_m$=5 m/s, $S$=1.14/1.32/1.51, $\Phi$=0.63, $D$=53 mm, $D_j$=2 mm, rim thickness=3.75 mm, $L$=90/150 mm, ncell=120,512). (a) Inlet boundary condition & $G$-field, (b) secondary-flow vectors at the cross-section containing the air-jets, (c) blowup of burner

# Effects of swirl strength and nozzle length ($\Phi$=0.63)

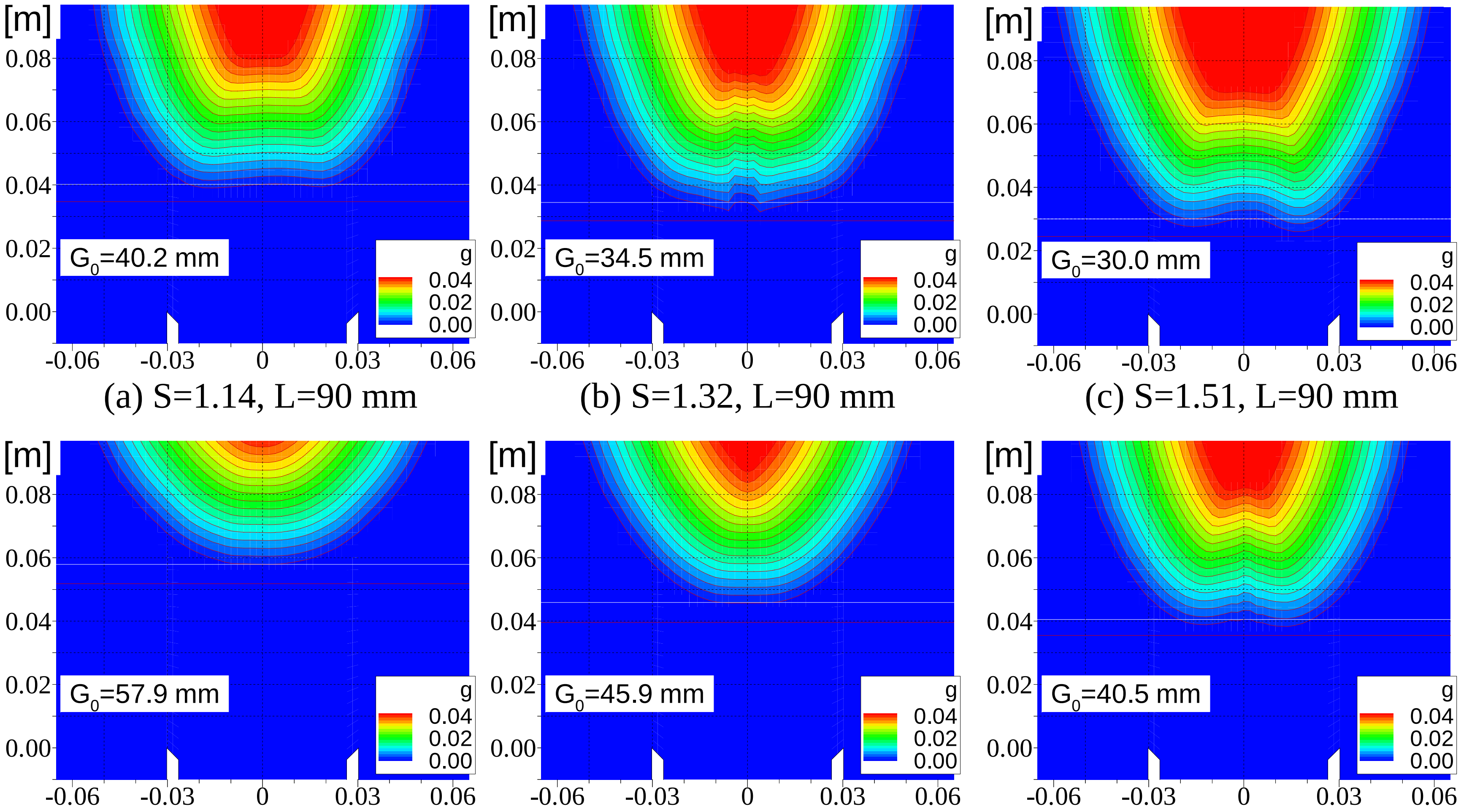


(a) S=1.14, L=90 mm (b) S=1.32, L=90 mm (c) S=1.51, L=90 mm

(d) S=1.14, L=150 mm (e) S=1.32, L=150 mm (f) S=1.51, L=150 mm

Comparison of *G*-fields for different swirl numbers (*S*=1.14/1.32/1.51) and nozzle lengths (*L*=90/150 mm). Red line: half of the maximum CH ; white line: bottom of the iso-surface $G=G_0$.

# Turbulent Premixed $CH_4$/Air Flame ($\Phi$=0.63) – CH radical & liftoff height

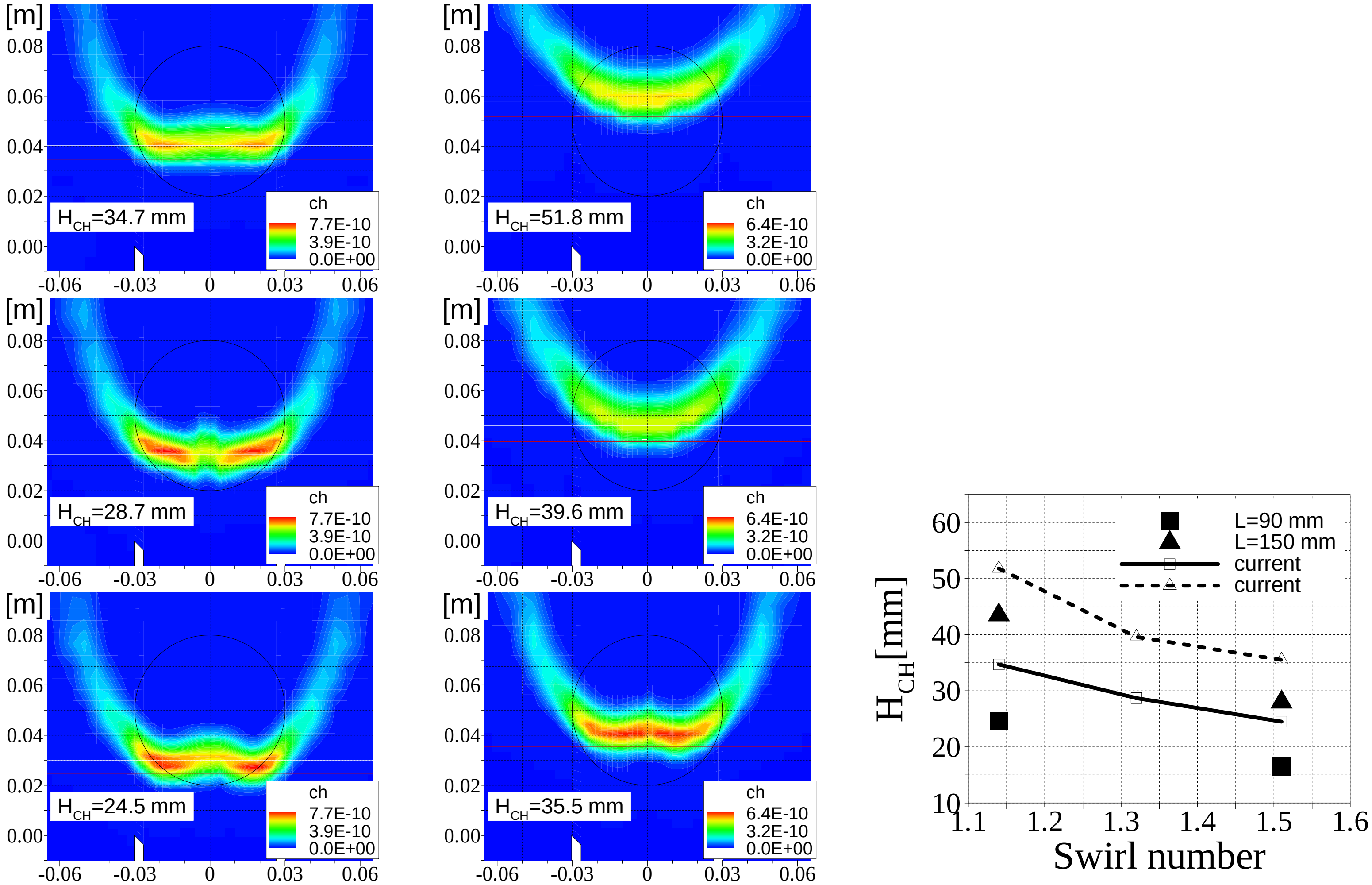


(a) $Y_{CH}$ ($L$=90 mm) (b) $Y_{CH}$ ($L$=150 mm) (c) Profiles of flame liftoff height

Comparison of CH radical distributions and flame liftoff heights for different swirl numbers ($S$=1.14/1.32,/1.51) and different nozzle lengths ($L$=90/150 mm): Red line denotes the liftoff height defined by the position of half of the maximum CH and white line by iso-surface $G$=$G_0$, respectively.

# Turbulent Premixed $CH_4$/Air Flame ($\Phi$=0.63) – centerline profiles

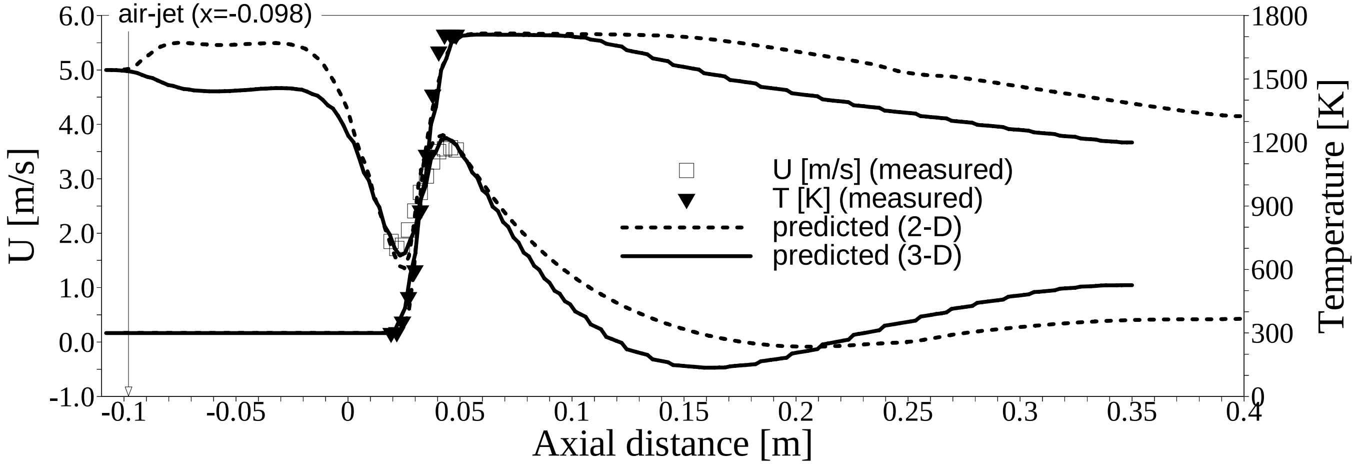


(a) in full distance

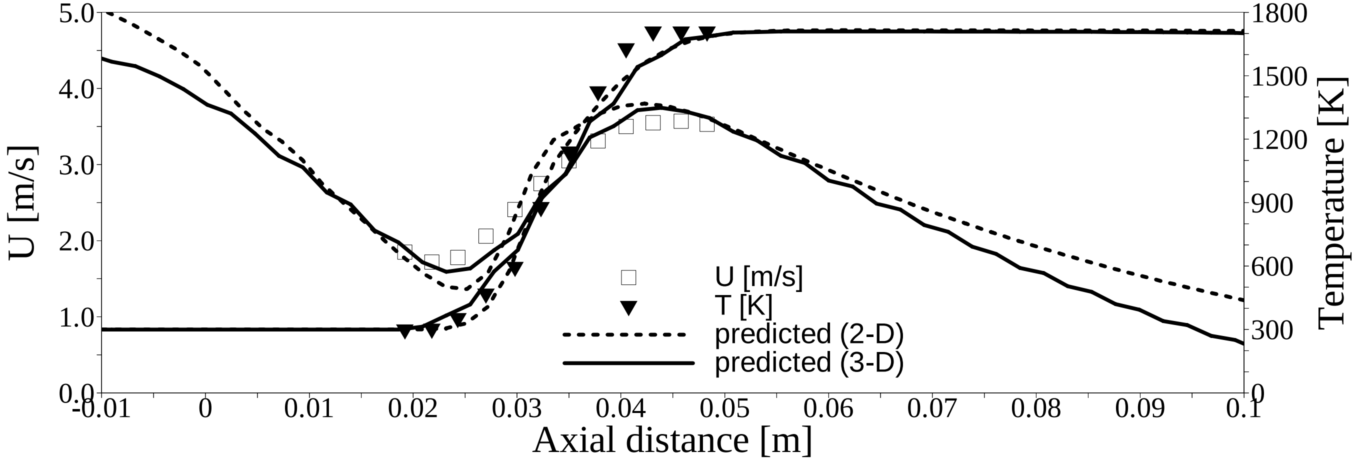


(b) near flame front

Centerline profiles of mean axial velocity and temperature ($U_m$=5 m/s, $S$=1.32 and $L$=90 mm). Symbols: Tachibana et al. 2004; lines: present prediction.

# Conclusion (1)

- **Numerical results clearly results indicate that the present level-set based flamelet approach has realistically simulated the structure and stabilization mechanism of the turbulent swirling stoichiometric and lean-premixed lifted flames in the low-swirl burner. In terms of the centerline velocity profiles and flame liftoff heights, the three-dimensional approach yields the much better conformity with agreements with measurements, compared to the two-dimensional approach.**

- **The flame lift-off height is decreased with increasing the swirl number. Around at the flame stabilization region, the elevated swirl strength leads to the decreased axial velocity due to the enhanced flow diverging effect and the increased turbulent flame speed corresponding to the increased turbulent intensity. At the axial location much closer to the nozzle exit, the decreased axial velocity is balanced with the increased turbulent flame speed. Thus, these two effects mainly control the flame lift-off height in the swirling premixed flames.**

# Conclusion (2)

- **The flame lift-off height is increased with increasing the nozzle length. This is directly tied with the decay of turbulence intensity along the nozzle downstream. Compared to the measured flame lift-off heights, the present approach slightly overestimates the flame lift-off heights for various swirl numbers and nozzle lengths. This discrepancy is mainly attributed to the shortcomings of the turbulence k-e model which might overestimate the decay of turbulence intensity in these swirling flames.**

- **Numerical results indicate that the predicted profiles are favorably well agreed with the experimental data for the centerline profiles of the mean axial velocity and reaction progress variable. However, at the reaction zone(0.04m$<$x$<$0.045m), there are the slight deviations which are responsible mainly for the defects of the turbulence k-e model as well as partially for the limitation of the present turbulent combustion model.**